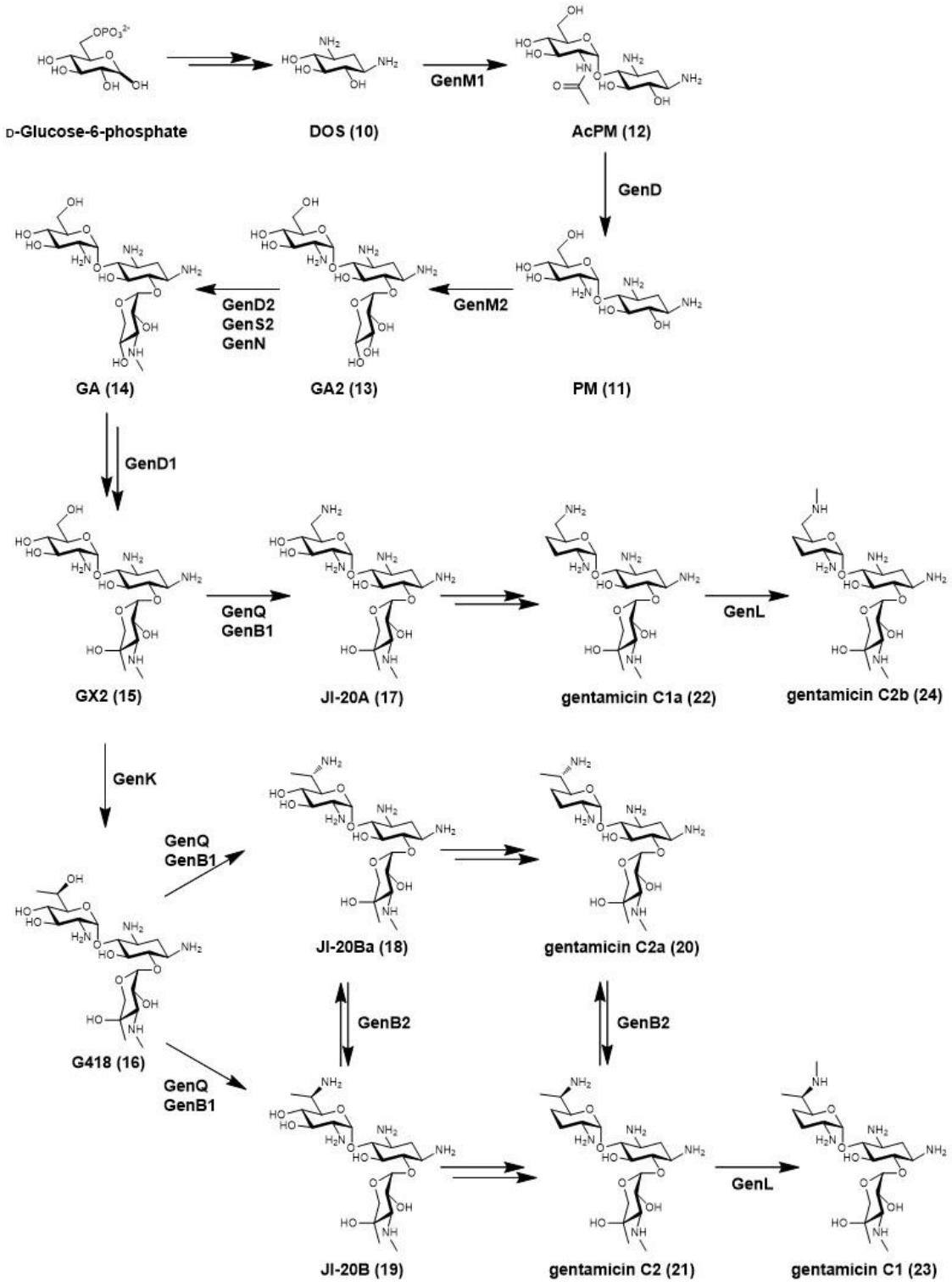

Supplementary Figure 1. The previously known biosynthetic pathway of gentamicin.

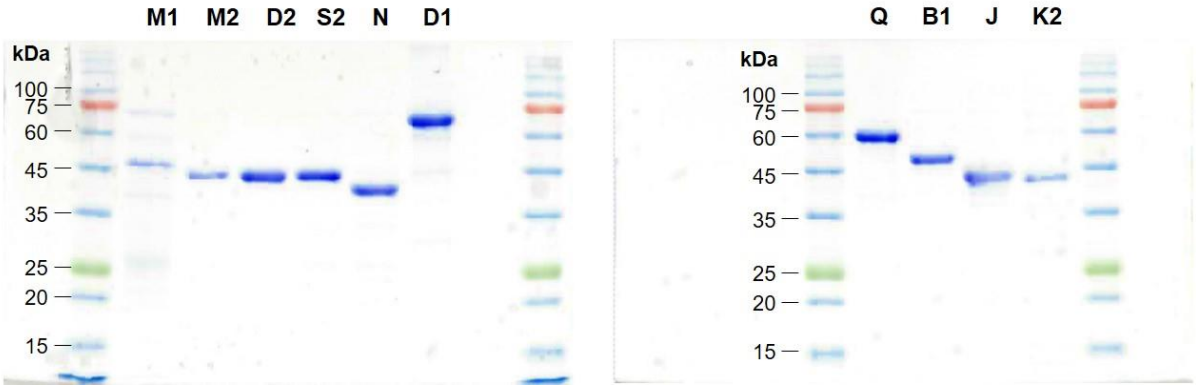

Supplementary Figure 2. SDS-PAGE of purified gentamicin biosynthetic enzymes. Gel is representative example of n>5 independent experiments.

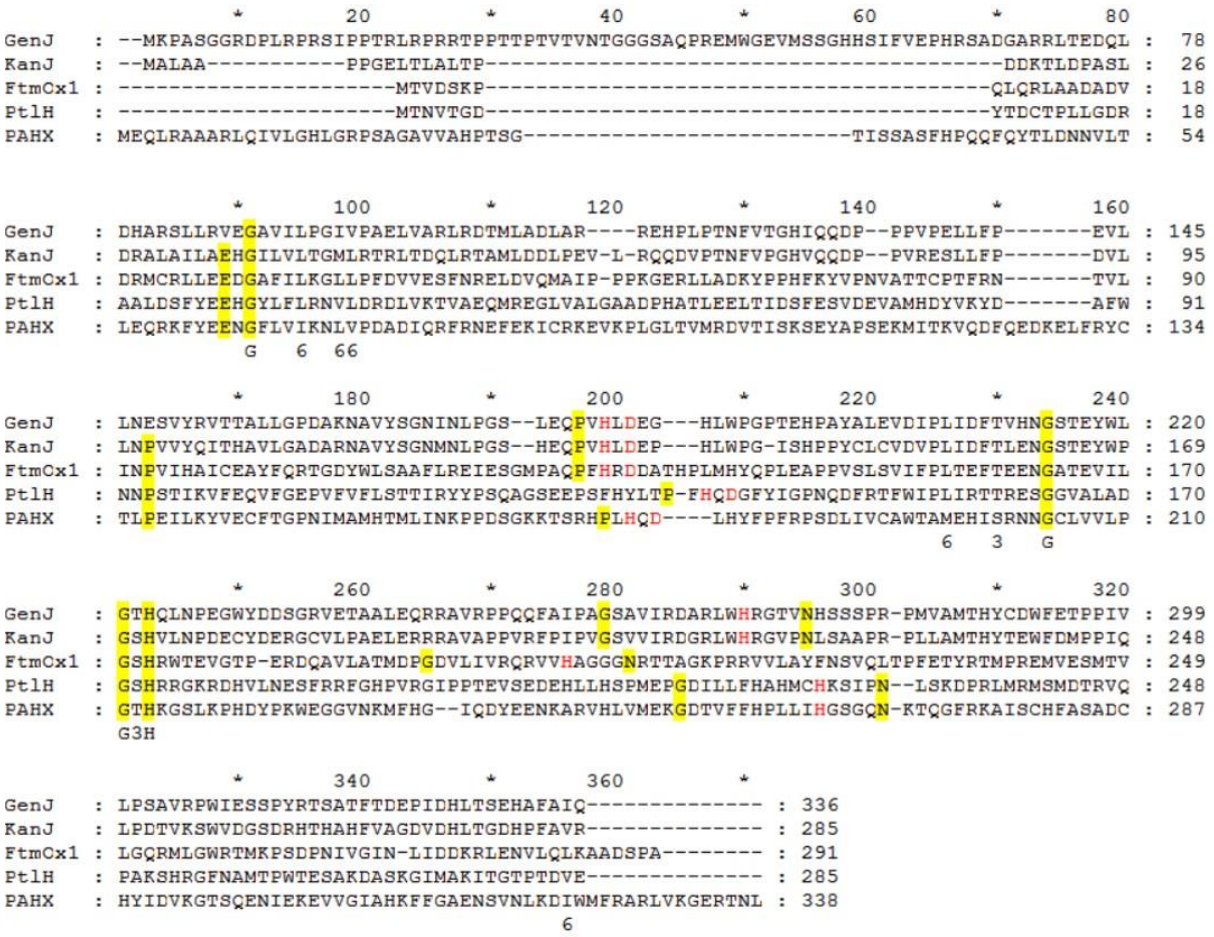

Supplementary Figure 3. Sequence alignment of GenJ with homologous other α-ketoglutarate dependent non-heme ion dioxygenases from *Streptomyces kanamyceticus* (KanJ: GenBank accession no. Q6L732), *Aspergillus fumigatus* (Ftm0x1: Q4WAW9.1), *Streptomyces avermitilis* (PtlH: BAC70702.2), *Homo sapiens* (PAHX: NP_006205.1). Multiple alignment of each sequence was carried out by clustalX. The highly conserved residues are represented in yellow boxes and Fe(II)-dependent binding motif HXD...H was marked in red.

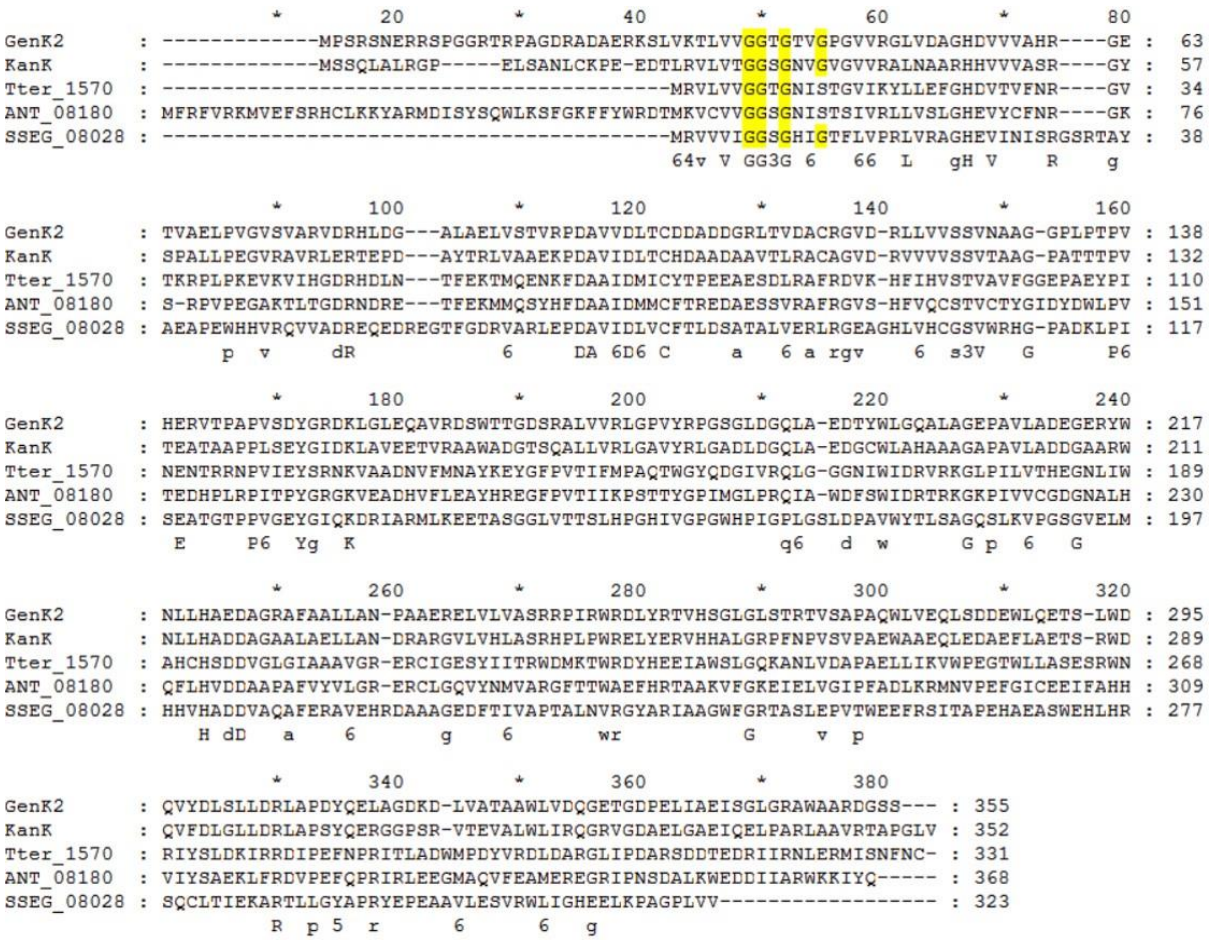

Supplementary Figure 4. Sequence alignment of GenK2 with homologous other NAD/NADP dependent dehydrogenases/reductases from *S. kanamyceticus* (KanK: GenBank accession no. Q2MFU6), *Thermobaculum terenum* ATCC BAA-198 (Tter_1570: ACZ42476), *Anaerolinea thermophile* UNI-1 (ANT_08180: BAJ62852), *Streptomyces sviceus* ATCC 29083 (SSEG_08028: EDY61449). Rossmann fold GGXGXXG NAD/NADP binding motif was conserved in yellow boxes.

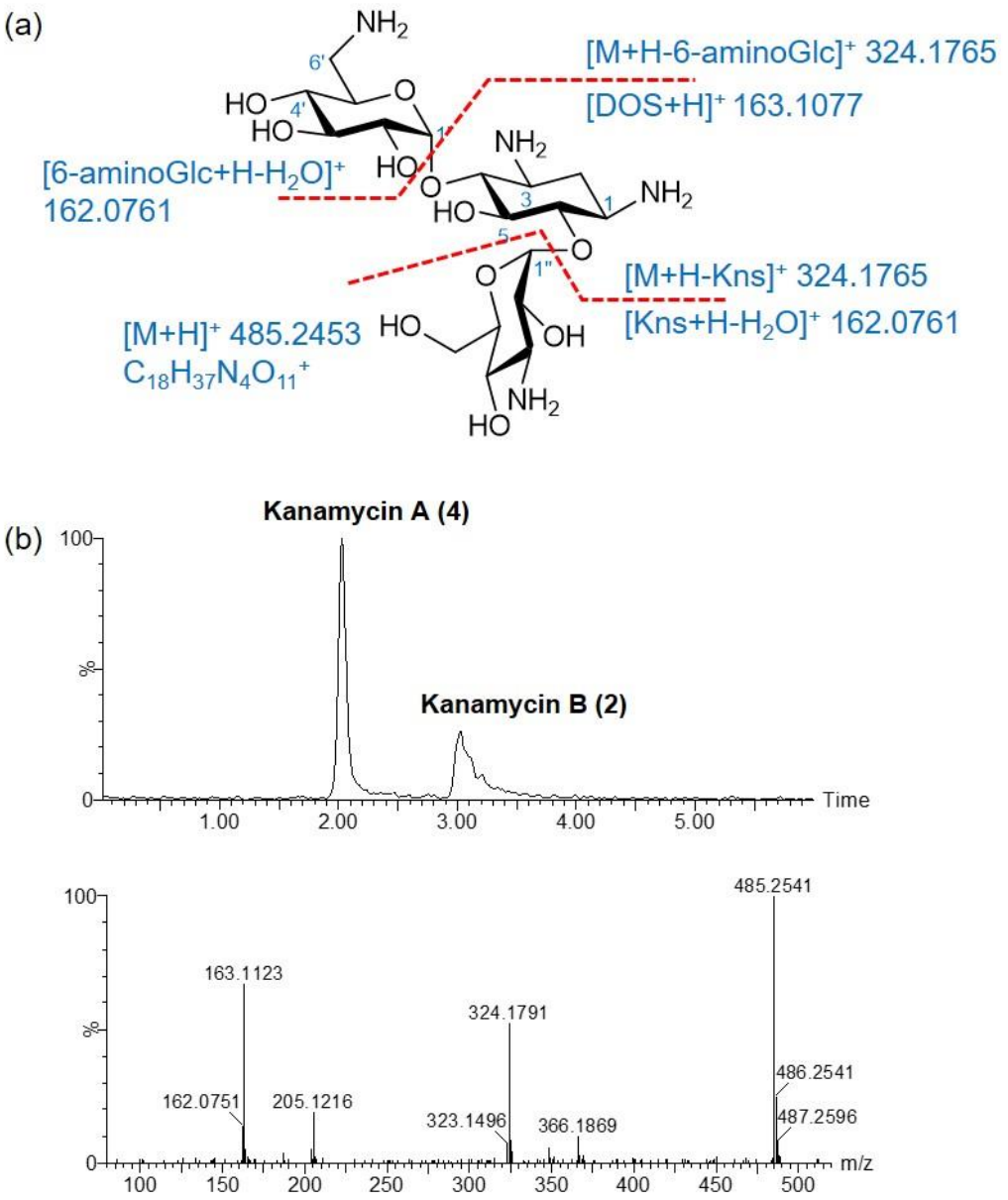

Supplementary Figure 5. GenJ-GenK2 reaction with kanamycin B (2). (**a**) MS/MS fragmentation pattern of kanamycin A (**4**). (**b**) The UPLC-qTOF-HR-MS chromatogram selected for *m/z* = 485.2453 and MS/MS spectra of enzymatically synthesized kanamycin A. The UPLC chromatogram and MS spectrum shown are representative examples of n>5 independent experiments.

(a)

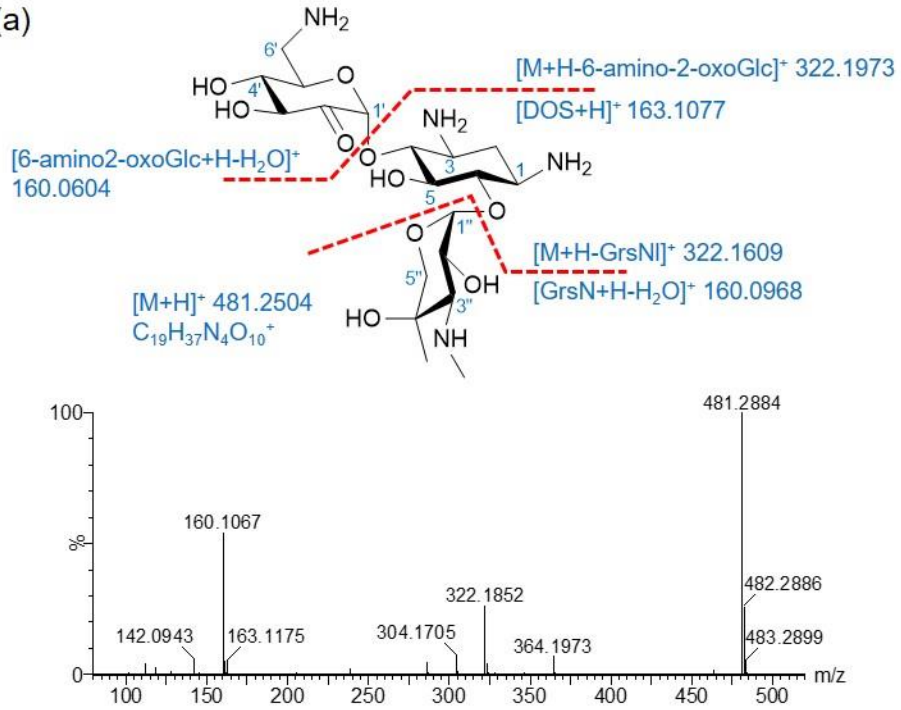
[M+H-6-amino-2-oxoGlc]+ 322.1973
[DOS+H]+ 163.1077
[6-amino2-oxoGlc+H-H2O]+
160.0604
[M+H-GrsNl]+ 322.1609
[GrsN+H-H2O]+ 160.0968
[M+H]+ 481.2504
C19H37N4O10+
481.2884
160.1067
322.1852
482.2886
142.0943
163.1175
304.1705
364.1973
483.2899
%
m/z

(b)

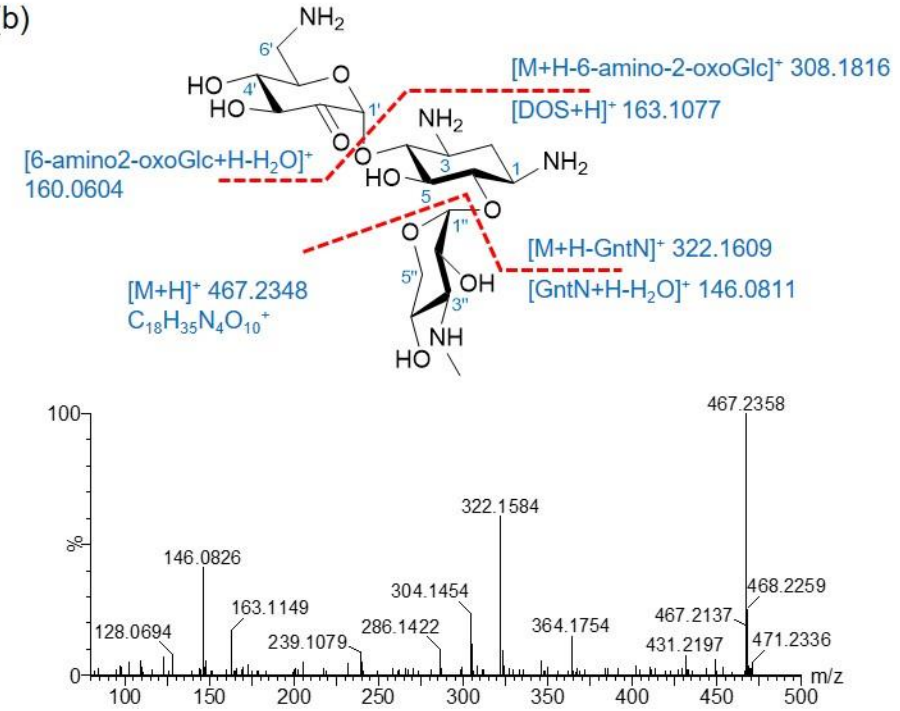
[M+H-6-amino-2-oxoGlc]+ 308.1816
[DOS+H]+ 163.1077
[6-amino2-oxoGlc+H-H2O]+
160.0604
[M+H-GntN]+ 322.1609
[GntN+H-H2O]+ 146.0811
[M+H]+ 467.2348
C18H35N4O10+
467.2358
322.1584
146.0826
304.1454
468.2259
163.1149
467.2137
128.0694
286.1422
364.1754
239.1079
431.2197
471.2336
%
m/z

(c)

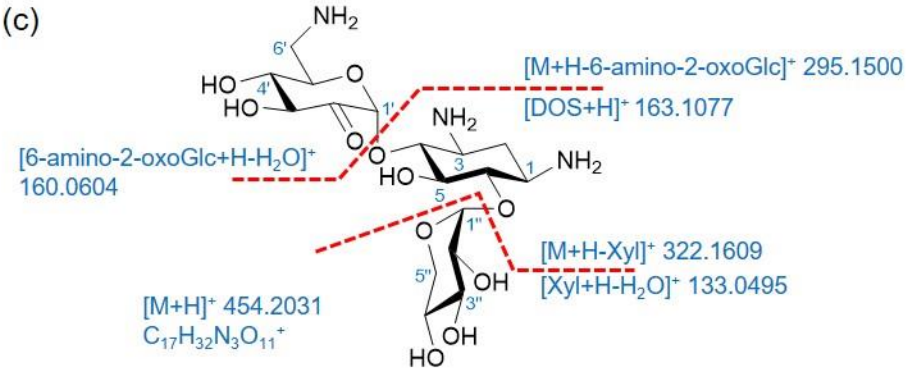
[M+H-6-amino-2-oxoGlc]+ 295.1500
[DOS+H]+ 163.1077
[6-amino-2-oxoGlc+H-H2O]+
160.0604
[M+H-Xyl]+ 322.1609
[Xyl+H-H2O]+ 133.0495
[M+H]+ 454.2031
C17H32N3O11+

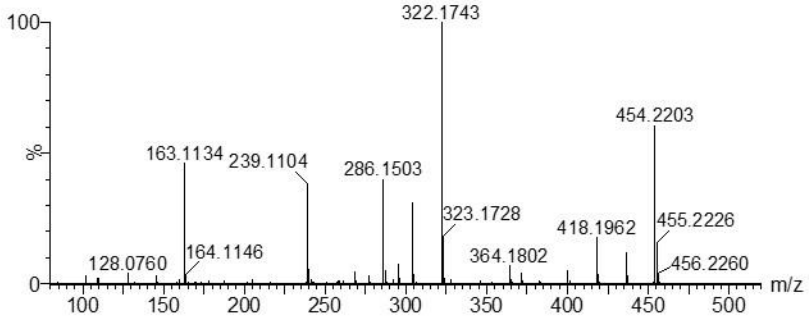
322.1743
454.2203
163.1134
239.1104
286.1503
323.1728
418.1962
455.2226
128.0760
164.1146
364.1802
456.2260
%
m/z

(d)

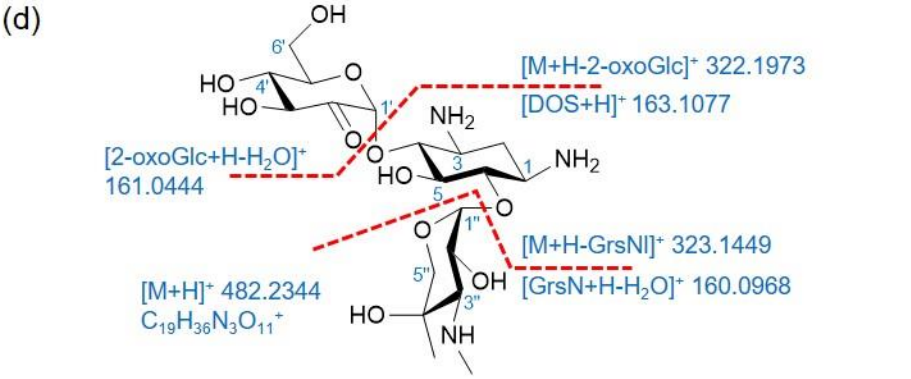
[M+H-2-oxoGlc]+ 322.1973
[DOS+H]+ 163.1077
[2-oxoGlc+H-H2O]+
161.0444
[M+H-GrsNl]+ 323.1449
[GrsN+H-H2O]+ 160.0968
[M+H]+ 482.2344
C19H36N3O11+

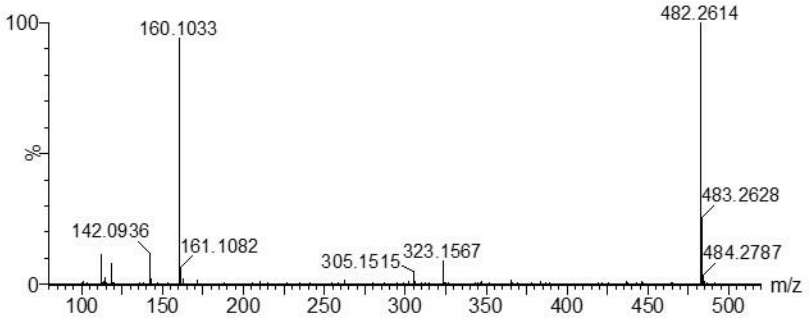
160.1033
482.2614
483.2628
142.0936
161.1082
305.1515
323.1567
484.2787
%
m/z

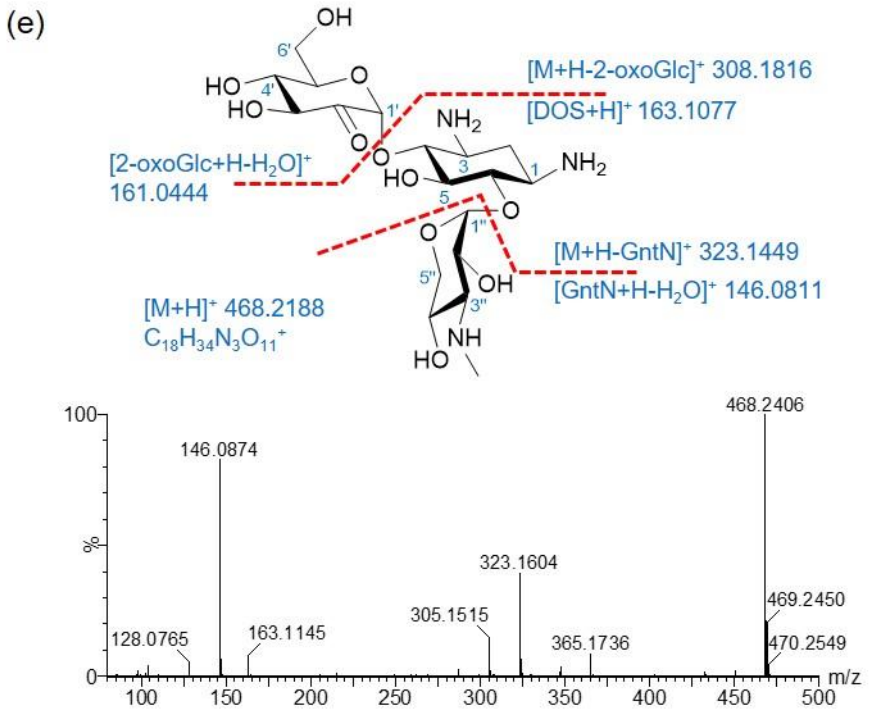

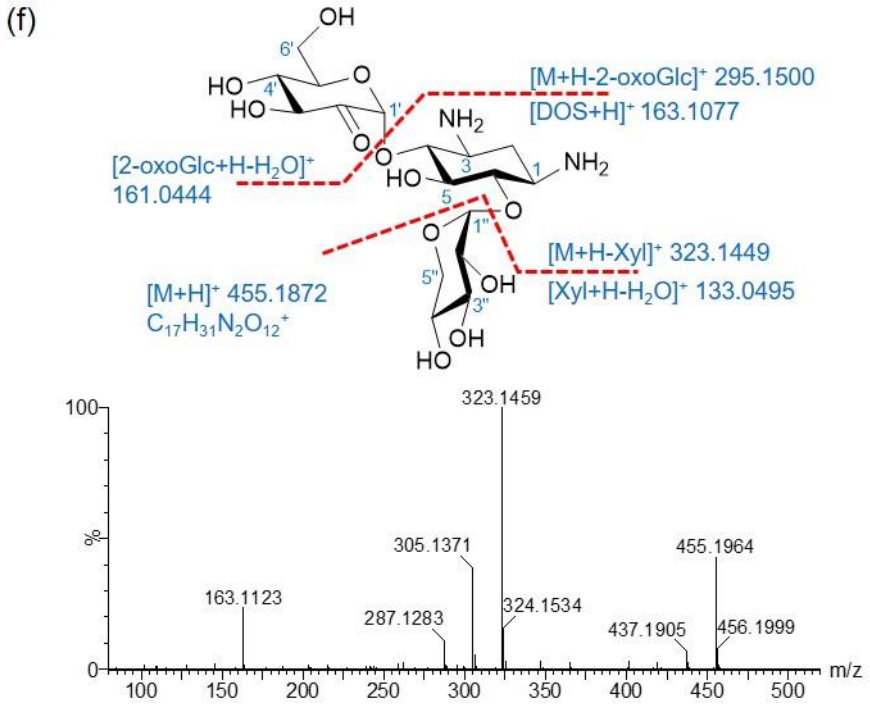

Supplementary Figure 6. The structural determination of 2′-oxo-JI-20A, 2′-oxo-6′AGA, 2′-oxo-6′AGA2, 2′-oxo-GX2, 2′-oxo-GA, and 2′-oxo-GA2. MS/MS fragmentation patterns and MS/MS spectra of enzymatically synthesized (**a**) 2′-oxo-JI-20A, (**b**) 2′-oxo-6′AGA, (**c**) 2′-oxo-6′AGA2, (**d**) 2′-oxo-GX2, (**e**) 2′-oxo-GA, and (**f**) 2′-oxo-GA2, respectively. The spectra shown are representative examples of n>5 independent experiments.

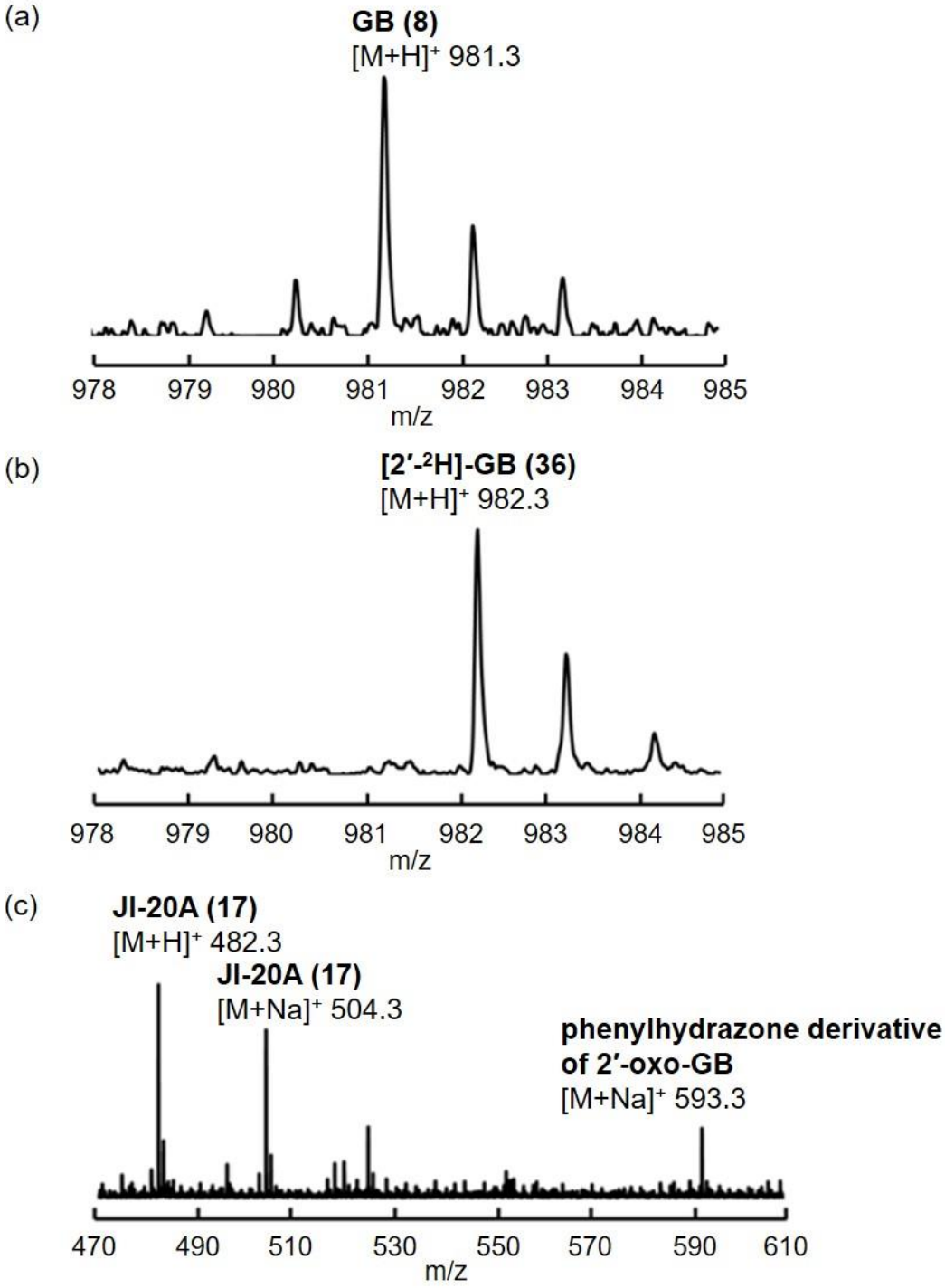

Supplementary Figure 7. **ESI-MS spectra of GenJ reaction with JI-20A (17) in the presence of (a) $NaBH_4$, (b) $NaBD_4$, and (c) phenylhydrazine.** $NaBH_4$ reduction: HR-MS $C_{37}H_{44}N_{10}O_{22}$ $[M+H]^+$ calc. 981.2704, obs. 981.2686[a]; $NaBD_4$ reduction: HR-MS $C_{37}H_{43}DN_{10}O_{22}$ $[M+H]^+$ calc. 982.2767, obs. 982.2716[a]; phenylhydrazine treatment: HR-MS $C_{25}H_{42}N_6O_9$ $[M+Na]^+$ calc. 593.2905, obs. 593.2931. The spectra shown are representative examples of $n>3$ independent experiments. ([a] All spectra were about dinitrophenyl (DNP) derivatives.)

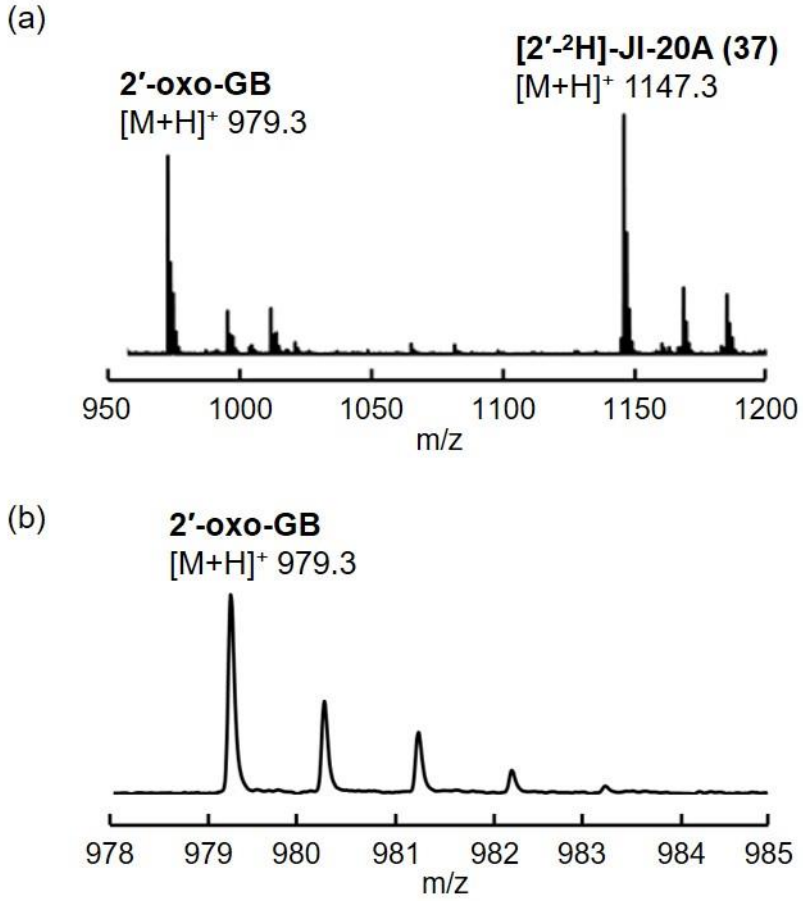

Supplementary Figure 8. GenJ-GenK2 reaction with [2′-^{2}H]-JI-20A (37). (**a**) ESI-MS spectra of the GenJ-GenK2 reaction with [2′-^{2}H]-JI-20A. (**b**) Expansion of the product. The spectra shown are representative examples of n>3 independent experiments. (All spectra were about dinitrophenyl (DNP) derivatives.)

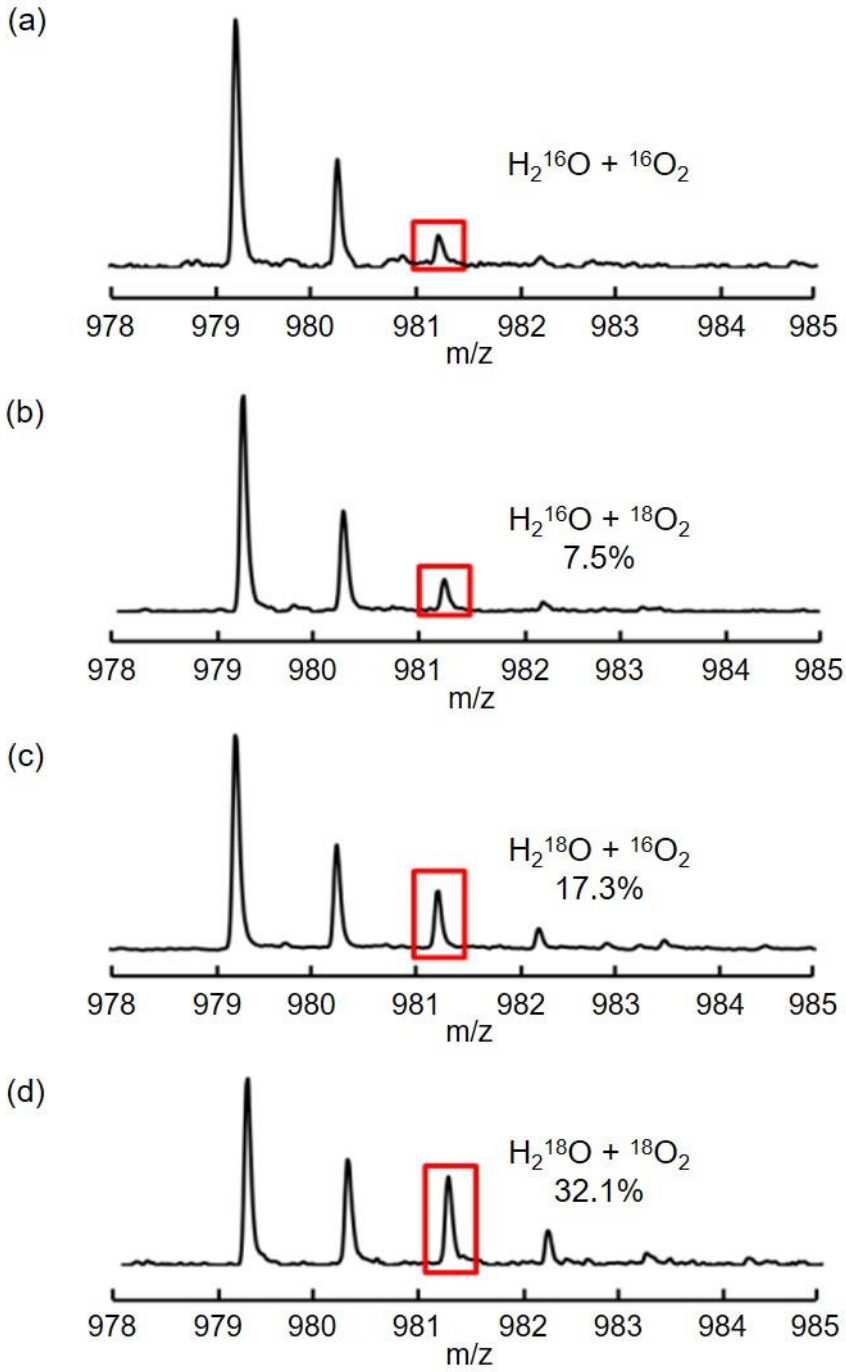

Supplementary Figure 9. ESI-MS spectra of GenJ reaction with (a) $^{16}O_2/H_2{}^{16}O$, (b) $^{18}O_2/H_2{}^{16}O$, (c) $^{16}O_2/H_2{}^{18}O$, and (d) $^{18}O_2/H_2{}^{18}O$. The spectra shown are representative examples of n>3 independent experiments. (All spectra were about dinitrophenyl (DNP) derivatives.)

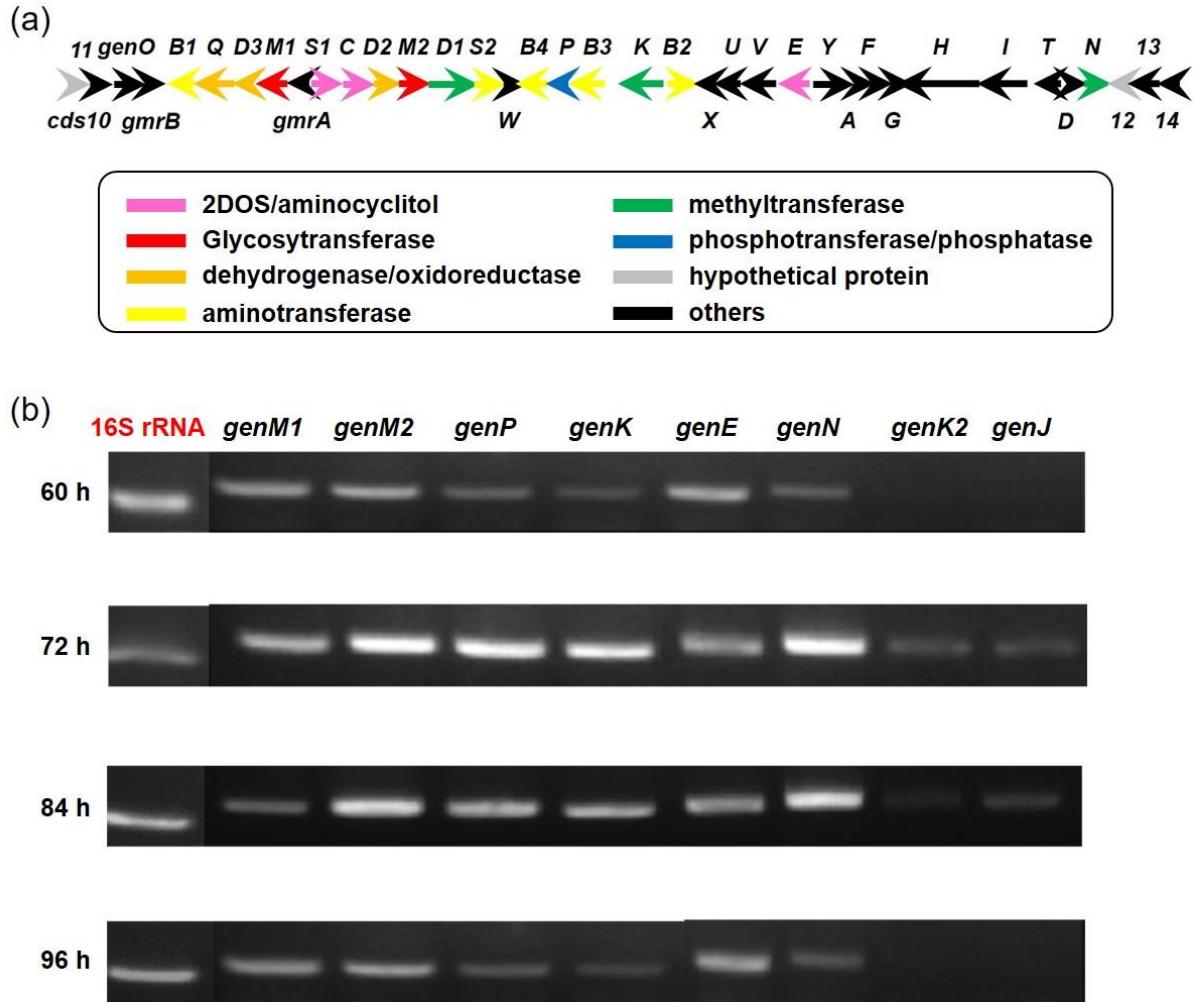

Supplementary Figure 10. Transcriptional analysis of six gentamicin biosynthetic genes and *genJ-genK2*. (**a**) Organization of gentamicin biosynthetic gene cluster from *Micromonospora echinospora* ATCC 15835. (**b**) Total RNAs were isolated from *M. echinospora* harvested after 60 h, 72 h, 84 h, and 96 h of cultivation. 16S rRNA gene was used as a control. Representative RT-PCR from at least three independent experiments are shown.

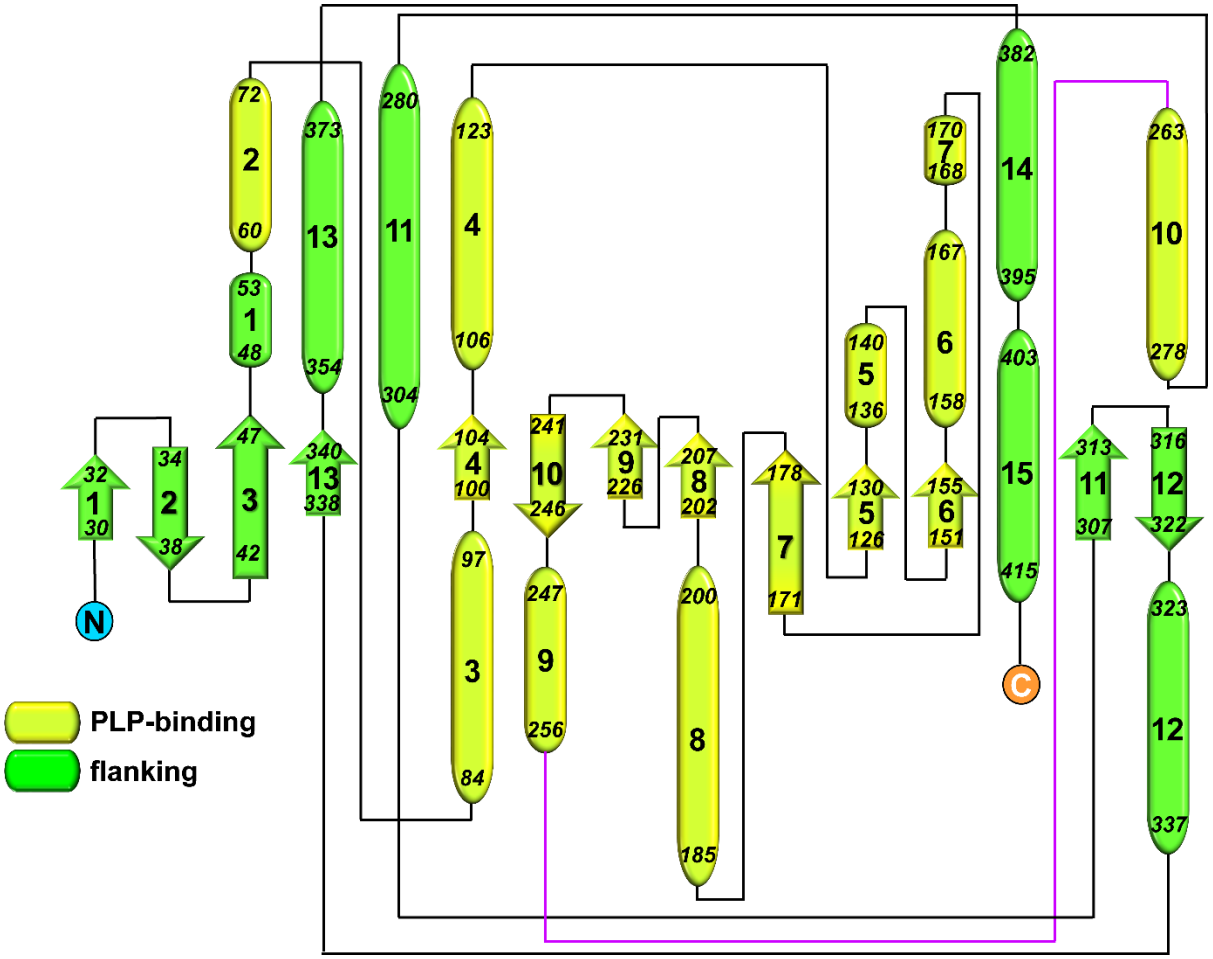

Supplementary Figure 11. Topological diagram of GenB1. The flanking domain and PLP-binding domain are shown in dark and light green, respectively. Secondary structure elements are indicated with helices and strands shown as cylinders and arrows, respectively. The connecting loop between α9 and α10 participating in the constitution of the active site of the other monomer is colored magenta and N-/C-termini are indicated by circles.

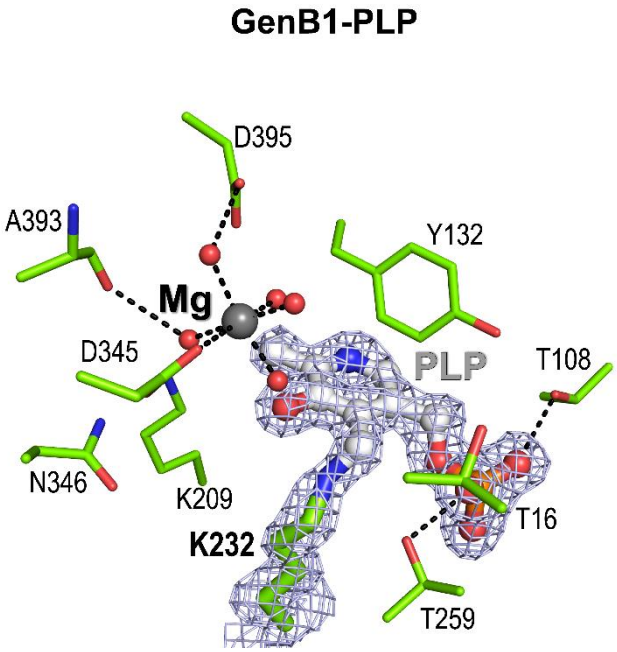

Supplementary Figure 12. Close-up view of the active site in holo-GenB1. 2*F*o-*F*c omit map (contoured at 1.0 σ) for the internal-aldimine formed between PLP (white) and Lys232 (green) shown in light blue mesh with ball-and-stick models. The electron density map was prepared by simulated annealing refinement of the final model with omission of PLP. Residues constituting the PLP-binding site are shown as green sticks. A magnesium ion and water molecules are indicated by gray and red spheres, respectively. Hydrogen bonds and ionic interactions are indicated by black dashed lines.

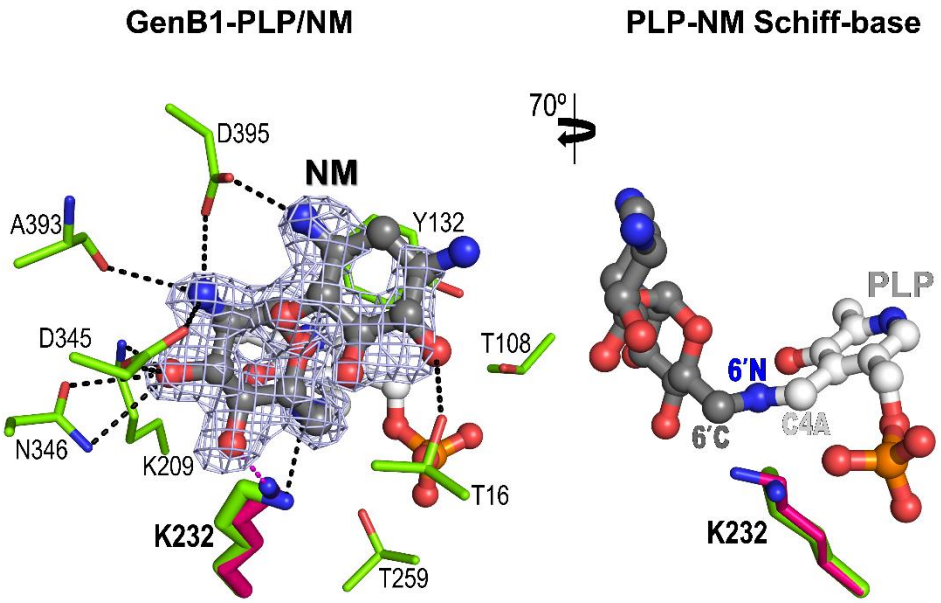

Supplementary Figure 13. Close-up view of the active site of holo-GenB1 in complex with NM (29). 2*Fo*-*Fc* omit map (contoured at 1.0 σ) for NM shown in light blue mesh with ball-and-stick models (left). Residues interacting with PLP and NM are shown as green sticks. Different conformations of Lys232 in each monomer are emphasized using thicker sticks colored in green and magenta, respectively. The view is rotated 70º for clarity, and the Schiff base intermediate formed between PLP and NM are shown (right). Atoms forming a covalent linkage are marked with labels (carbon (6′C) and nitrogen (6′N) of NM, and carbon (C4A) of PLP). Hydrogen bonds and ionic interactions are indicated by black dashed lines.

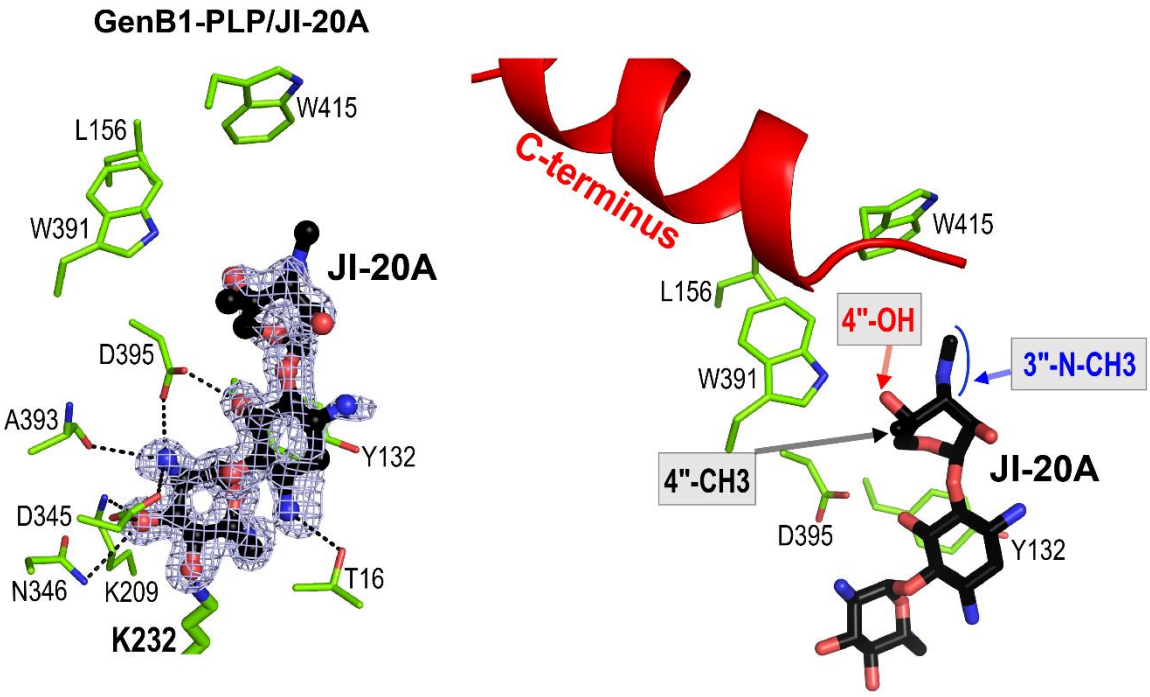

Supplementary Figure 14. Close-up view of the active site of holo-GenB1 in complex with JI-20A (17). 2*F*o-*F*c omit map (contoured at 1.0 σ) for JI-20A shown in light blue mesh with ball-and-stick models (left). Residues interacting with JI-20A are shown as green sticks. Residues involved in hydrophobic contacts (within 5Å) are presented by sticks. The moieties of ring III are labeled in gray boxes (right). The C-terminus at the methyl pocket is shown as a red ribbon model. For brevity, PLP is not shown in this figure. Hydrogen bonds and ionic interactions are indicated by black dashed lines.

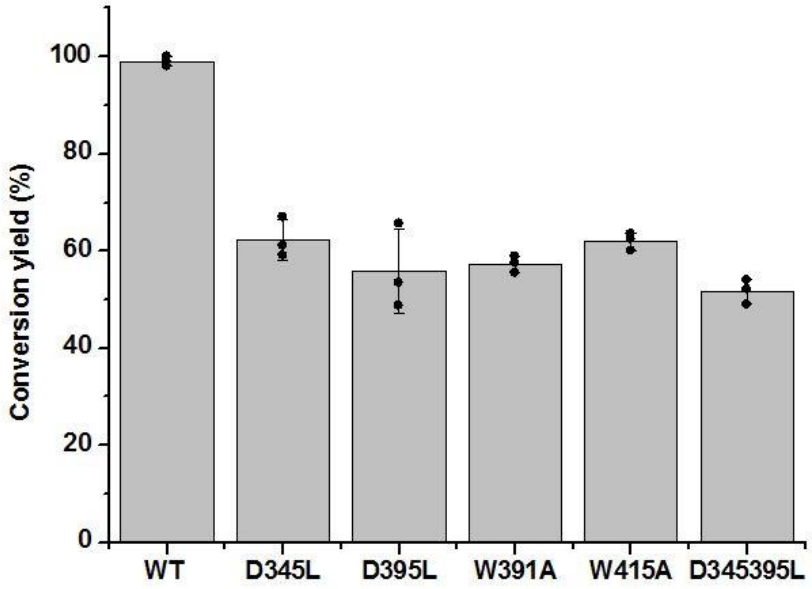

Supplementary Figure 15. Relative enzymatic activities of GenB1 mutants. The Y-axis represents the C6′-amination activity toward GX2 (**15**) when the wild-type and the mutant proteins of GenB1 were respectively incubated with GenQ and GX2. Data are expressed as means (n=3) ± standard deviations from three independent experiments.

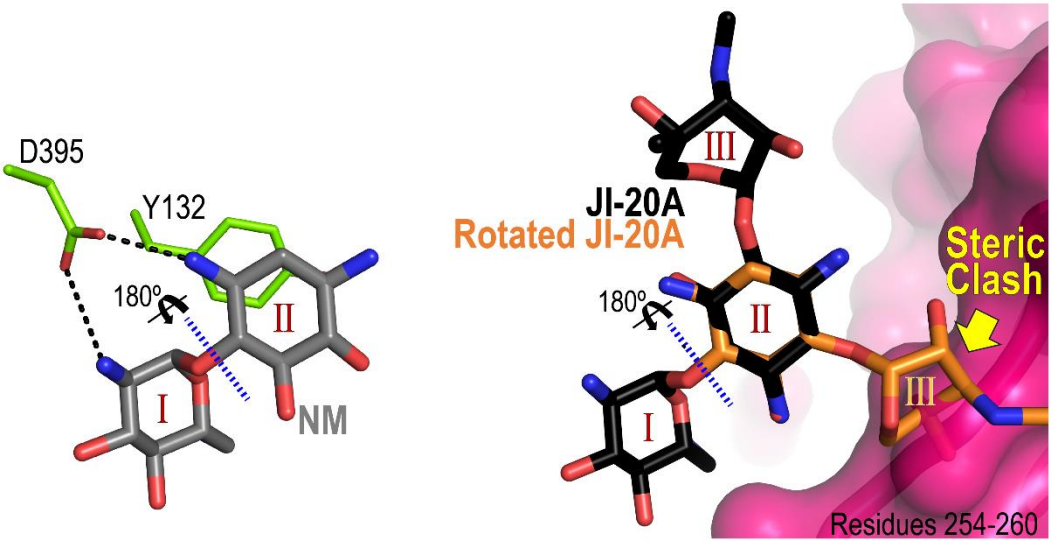

Supplementary Figure 16. The flipping of ring II in JI-20A (17). NM (**29**) (gray) and JI-20A (black) bound to GenB1 are shown as stick models (left and right). The three sugar rings of JI-20A are labeled in red Roman Numerals (I-III). Two residues (Try132 and Asp395) forming the C-H/π stacking and charge interactions with ring II are shown as green sticks. Orange-colored JI-20A in the right is artificially generated by rotating black-colored JI-20A about the linkage between ring I-II to match the ring II of JI-20A with that of NM (left). Steric clash between the rotated JI-20A and the active site is indicated by a yellow arrow. Hydrogen bonds and ionic interactions are indicated by black dashed lines.

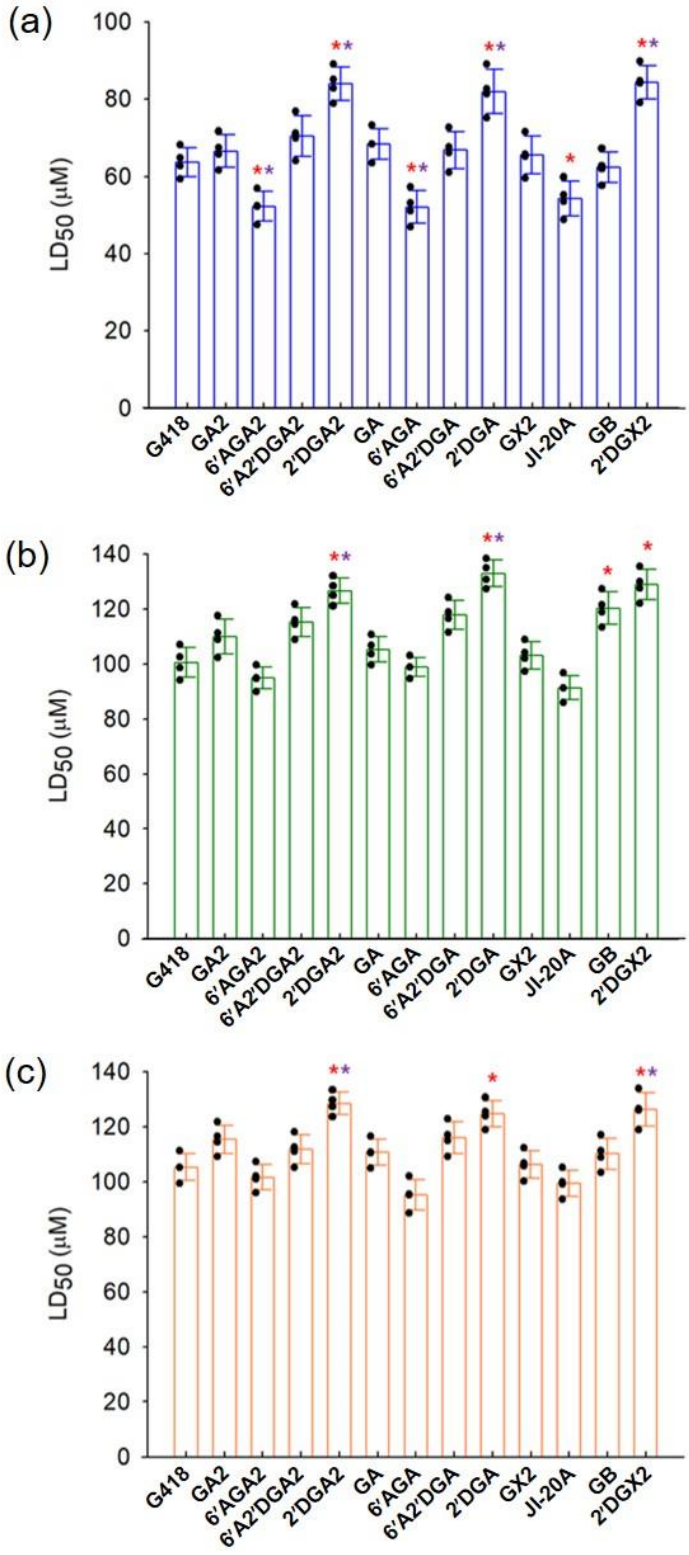

Supplementary Figure 17. Cytotoxicity of gentamicin intermediates against three different mammalian renal cell lines. (**a**) LD_{50} (μM) of G418 (**16**), GA2 analogs (GA2 (**13**), 6′AGA2 (**34**), 6′A2′DGA2 (**31**), and 2′DGA2 (**25**)), GA analogs (GA (**14**), 6′AGA (**35**), 6′A2′DGA (**32**), and 2′DGA (**26**)), and GX2 analogs (GX2 (**15**), JI-20A (**17**), GB (**8**), and 2′DGX2 (**27**)) against HEK-293 cells. (**b**) LD_{50} (μM) of G418, GA2 analogs, GA analogs, and GX2 analogs against LLC-PK1 cells. (**c**) LD_{50} (μM) of G418, GA2 analogs, GA analogs, and GX2 analogs

against COS-7 cells. Data were expressed as means (n=4) ± standard deviations and tested for significance using paired or unpaired two-tailed t-test with analysis of variance as appropriate. n indicates biologically independent experiments. Results with $P<0.01$ were considered significant. *$P<0.01$ *vs* G418; *$P<0.01$ *vs* series. The precise p-values are: (**a**) between 6′AGA2-treated HEK-293 samples and G418-treated samples: 1e-5; between 2′DGA2-treated samples and G418-treated samples: 1e-7; between 6′AGA-treated samples and G418-treated samples: 1e-5; between 2′DGA-treated samples and G418-treated samples: 2e-7; between JI-20A-treated samples and G418-treated samples: 1e-4; between 2′DGX2-treated samples and G418-treated samples: 2e-8; (**b**) between 2′DGA2-treated LLC-PK1 samples and G418-treated samples: 2e-7; between 2′DGA-treated samples and G418-treated samples: 1e-8; between GB-treated samples and G418-treated samples: 2e-4; between 2′DGX2-treated samples and G418-treated samples: 2e-8; (**c**) between 2′DGA2-treated COS-7 samples and G418-treated samples: 1e-8; between 2′DGA-treated samples and G418-treated samples: 2e-7; between 2′DGX2-treated samples and G418-treated samples: 1e-7.

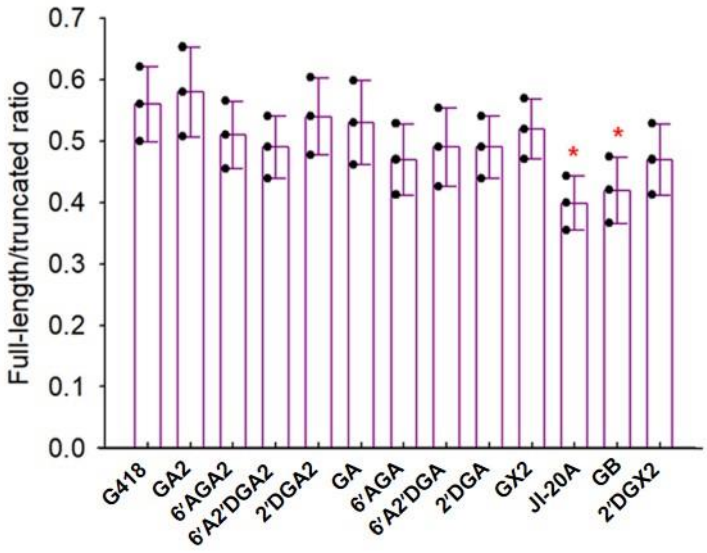

Supplementary Figure 18. Comparative PTC read-through activity of gentamicin intermediates against primary human cystic fibrosis bronchial epithelial cells. G418 (**16**), GA2 analogs (GA2 (**13**), 6′AGA2 (**34**), 6′A2′DGA2 (**31**), and 2′DGA2 (**25**)), GA analogs (GA (**14**), 6′AGA (**35**), 6′A2′DGA (**32**), and 2′DGA (**26**)), and GX2 analogs (GX2 (**15**), JI-20A (**17**), GB (**8**), and 2′DGX2 (**27**)) were treated at 25 μM. The ratio of full-length to truncated CFTR expressed in the gentamicin intermediates-exposed cells was determined by size exclusion chromatography with MS, described hereinabove. Data were expressed as means (n=3) ± standard deviations and tested for significance using paired or unpaired two-tailed t-test with analysis of variance as appropriate. n indicates biologically independent experiments. Results with $P<0.01$ were considered significant. *$P<0.01$ *vs* G418. Below are specific p-values between treatments: between JI-20A-treated HEK293 samples and G418-treated samples: 1e-7; between GB-treated samples and G418-treated samples: 2e-6.

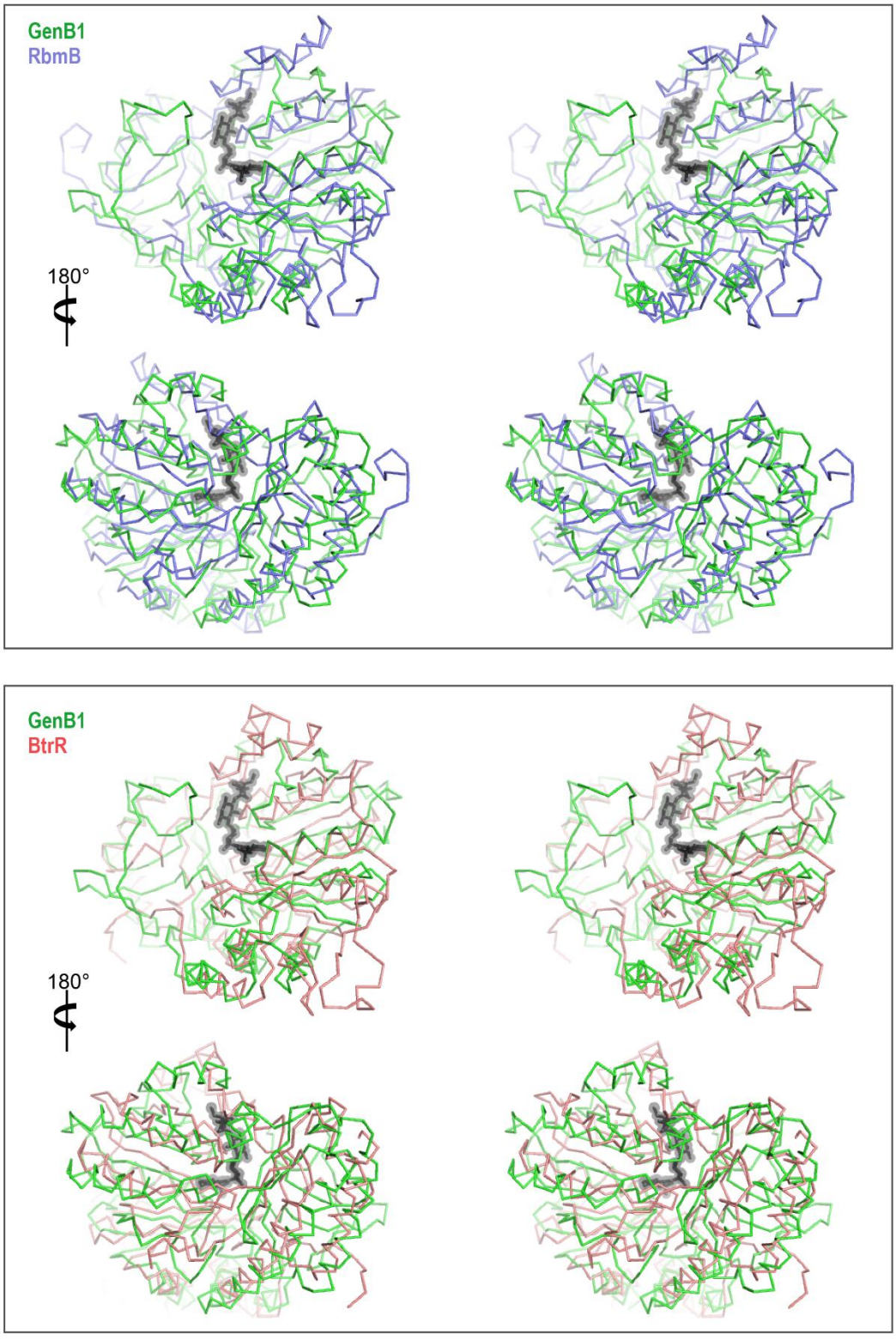

Supplementary Figure 19. Stereo view of the superimposed Cα tracing of GenB1 (green), RbmB (slat: PDB entry 5W70), and BtrR (salmon: PDB entry 5W71). JI-20A (**17**) bound to the active site of GenB1 is shown as ball and stick models.

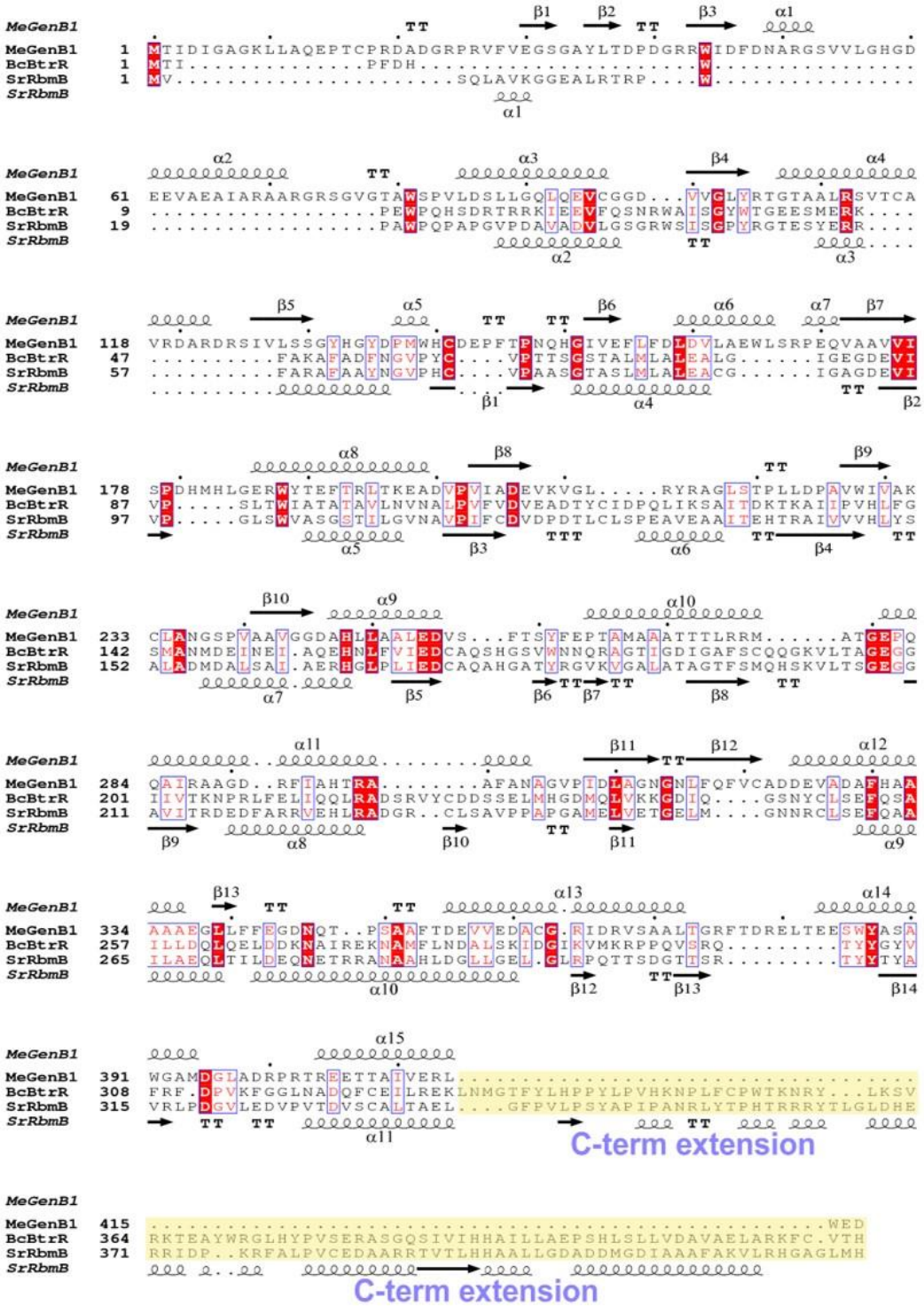

Supplementary Figure 20. Structure-based sequence alignments of GenB1, BtrR, and RbmB. Secondary structure assignments in the top and bottom correspond to GenB1 and RbmB, respectively. Identical residues are highlighted with red backgrounds and conserved residues are indicated by red letters in blue boxes. C-terminal extensions observed in BtrR and RbmB are highlighted in yellow backgrounds. Expasy numbers of the aligned GenB1, BtrR, and RbmB are as follows: GenB1 from *M. echinospora* (Q70KD9), BtrR from *Bacillus circulans* (Q8G8Y2), and RbmB from *Streptomyces ribosidificus* (Q4R0W2). This figure is generated by using ESPript.

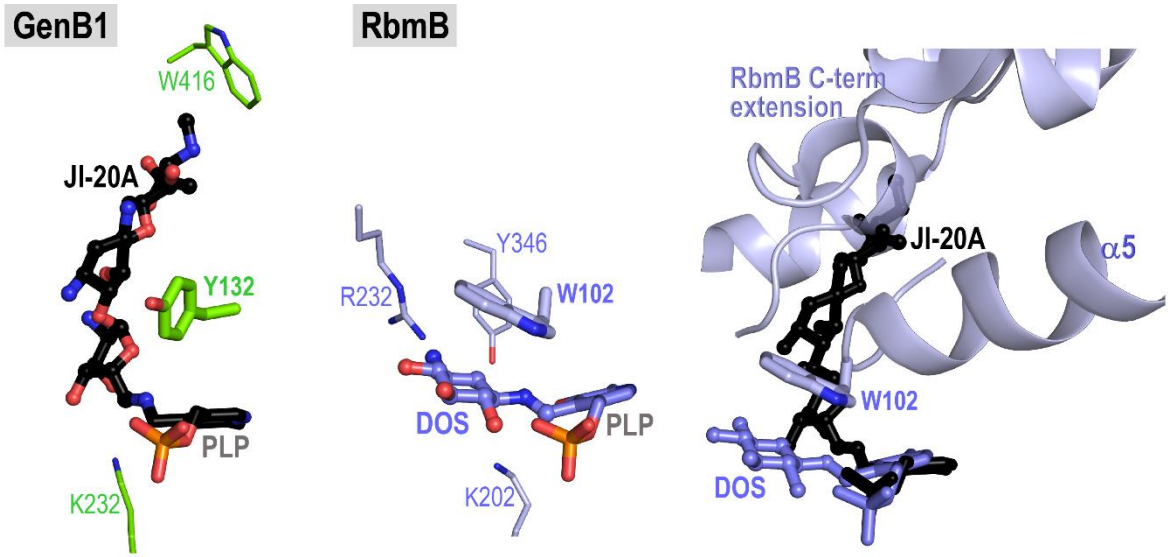

Supplementary Figure 21. Comparison of active sites between GenB1 and RbmB. Key residues determining the size and shape of the active site for JI-20A (**17**) (black) and DOS (**10**) (slat) are shown as stick models (left and middle). Residues (Tyr132 in GenB1 and Trp102 in RbmB (PDB entry 5W70)) forming the aromatic platform are emphasized using thicker sticks. Color-coding for PLPs is identical to their linked products. Superposition of the active sites between holo-GenB1 complexed with JI-20A and holo-RbmB complexed with DOS is shown as ribbon and stick model (right). For clarity, GenB1 is not shown. Clash of JI-20A with the active site of RmbB clearly shows that the active site of RbmB cannot accommodate JI-20A. The crystal structures of BtrR and RbmB are superposed with rmsd of 1.89 Å for 358 corresponding Cα atoms. Due to this high structural resemblance, BtrR is not presented in this figure for brevity.

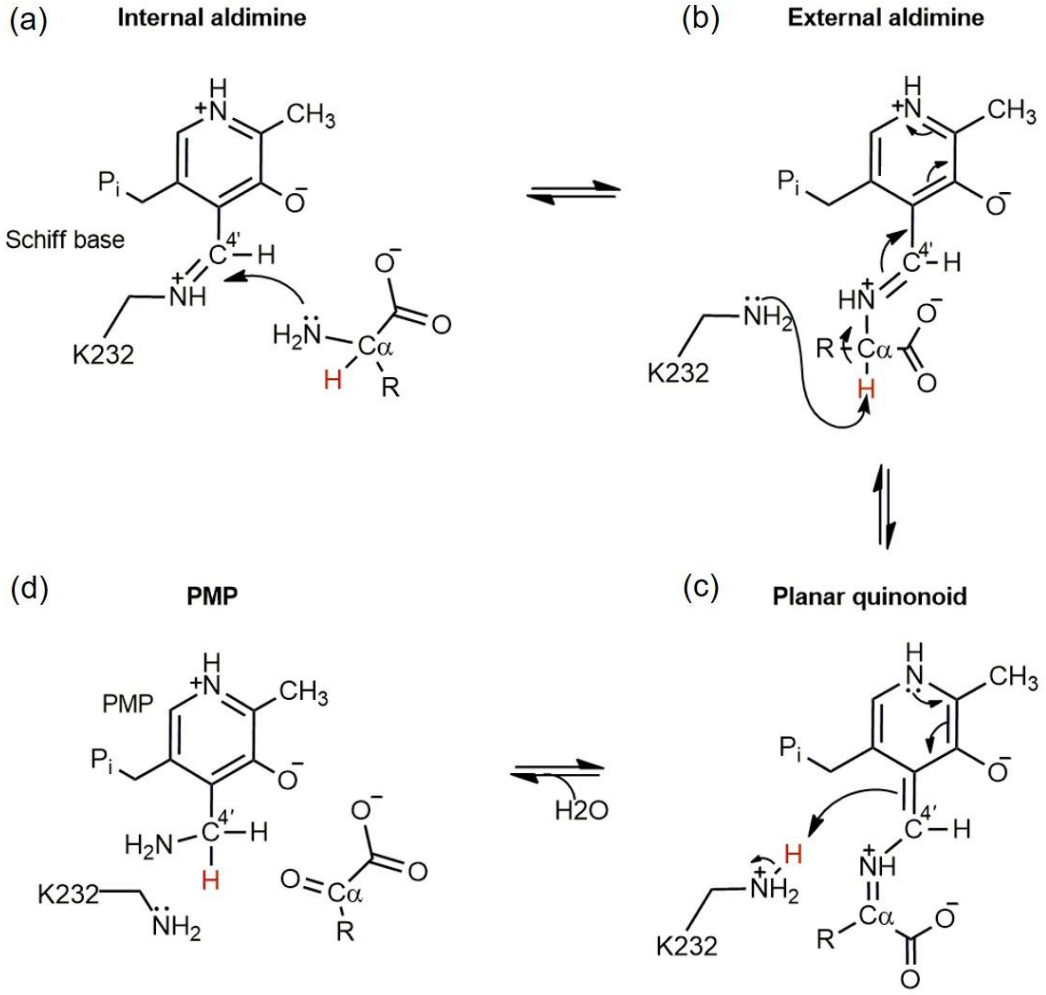

Supplementary Figure 22. General transamination reaction mechanism. This figure shows the transfer of an amino group in a donor substrate to PLP to form PMP. (**a**) At the resting state in transaminases, the C4′ atom of PLP is linked to the ε-amino group of a lysine residue through a Schiff base (internal aldimine). (**b**) The amino nitrogen atom of the incoming donor substrate replaces the lysine nitrogen atom to form the external aldimine. (**c**) The displaced lysine residue abstracts a proton from the C_α atom in the donor substrate and attaches the proton to the C4′ atom of PLP, which changes the location of the Schiff base: the C4′=N Schiff base is changed to the C_α=N Schiff base in the external aldimine intermediate to form planar quinonoid. (**d**) The hydrolysis of the C_α=N bond results in the formation of the pyridoxamine phosphate (PMP). The next transfer of the amino group in PMP to an acceptor molecule occurs in the exact reversal way. The carbonyl carbon of the acceptor substrate is attacked by the amino group at the C4′atom of PMP to form the external aldimine. This time the same lysine residue transfers a proton from the C4′ atom to the carbonyl carbon of the acceptor substrate to generate a Schiff base between the C4′ atom and the amino group. The hydrolysis of this Schiff base gives rise to an aminated product. K232 indicates the lysine residues for proton transfer in GenB1. The C_α proton is highlighted in red.

Supplementary Table 1. Incorporation of ^{18}O into JI-20A (17) from molecular $^{18}O_2$ and $H_2{}^{18}O$ during the GenJ reaction. Representative data from n=3 independent experiments are shown.

Conditions	*m/z* 979	*m/z* 980	*m/z* 981	*m/z* 982	Incorporation [%]
Calc.	100	45.0	14.4	3.5	
$^{16}O_2/H_2{}^{16}O$	100	42.5	14.0	3.1	0
$^{18}O_2/H_2{}^{16}O$	100	42.3	21.9	6.8	7.5
$^{16}O_2/H_2{}^{18}O$	100	51.9	31.7	9.4	17.3
$^{18}O_2/H_2{}^{18}O$	100	56.5	46.6	18.2	32.1

All spectra were about dinitrophenyl (DNP) derivatives.

Supplementary Table 2. Crystallographic data and Refinement statistics of GenB1 from *M. echinospora*

	GenB1_Se	GenB1_PLP	GenB1_ PLP/NM (29)	GenB1_ PLP/JI-20A (17)
Data collection				
X-ray source	PLS_5C	PLS_7A	PLS_5C	PLS_7A
Wavelength (Å)	Peak_0.97930	1.00003	0.97960	0.97934
Space group	$P2_12_12_1$	$P2_12_12_1$	$P2_12_12_1$	$P2_12_12_1$
Cell dimensions				
a, *b*, *c* (Å)	76.27, 87.61, 113.07	77.14, 88.01, 116.14	77.85, 89.16, 117.36	77.77, 88.69, 116.85
α, β, γ (°)	90, 90, 90	90, 90, 90	90, 90, 90	90, 90, 90
Resolution (Å)	50-1.80 (1.83-1.80)*	50-1.70 (1.73-1.70)	50-1.76 (1.79-1.76)	50-1.40 (1.42-1.40)
R_{merge} (%)	0.113 (0.239)	0.055 (0.241)	0.069 (0.299)	0.052 (0.325)
$I/\sigma I$	15.9 (8.4)	34.0 (3.6)	28.6 (4.2)	37.1 (3.0)
Completeness (%)	97.9 (91.6)	97.2 (82.4)	92.2 (59.0)	92.0 (60.7)
Redundancy	8.3 (5.1)	9.4 (4.0)	9.5 (4.9)	9.8 (4.5)
Refinement				
Resolution (Å)		33.80-1.70	32.30-1.76	27.39-1.40
No. reflections		84719	74621	144352
R_{work} / R_{free} (%)		0.160/0.192	0.183/0.230	0.172/0.193
No. atoms				
Protein		6212	6212	6212
Ligand/ion		32	74	96
Water		684	626	967
Average *B*-factor (Å^2)				
Protein		14.65	19.79	17.59
Ligand/ion		9.70	21.03	26.95
Water		21.09	26.04	28.21
R.m.s deviations				
Bond lengths (Å)		0.012	0.007	0.009
Bond angles (º)		1.13	0.89	0.75

Each dataset was collected from a single crystal. *Values in parentheses are for highest-resolution shell.

Supplementary Table 3. Antibacterial activity of gentamicin biosynthetic intermediates. Representative data from n=3 independent experiments are shown.

gentamicin intermediates		MIC (μg/mℓ)							
		Type strain				Clinical isolate			
		E. faecalis ATCC 29212	*P. aeruginosa* ATCC 27853	*S. aureus* ATCC 29213	*E. coli* ATCC 25922	*E. faecalis* CCARM 5025	*P. aeruginosa* CCARM 2002	*S. aureus* CCARM 3180	*E. coli* CCARM 1085
gentamicin (QC)		16	1–2	1	0.5–1	>128	>128	>128	16
GA2 analogs	GA2	>128	>128	>128	>128	>128	>128	>128	>128
	6′AGA2	>128	>128	>128	64	>128	>128	>128	>128
	6′A2′DGA2	>128	>128	>128	>128	>128	>128	>128	>128
	2′DGA2	>128	>128	>128	>128	>128	>128	>128	>128
GA analogs	GA	>128	>128	128	128	>128	>128	>128	>128
	6′AGA	>128	>128	8	8	>128	>128	>128	>128
	6′A2′DGA	>128	>128	16	16	>128	>128	>128	>128
	2′DGA	>128	>128	>128	>128	>128	>128	>128	>128
GX2 analogs	GX2	>128	>128	32	32	>128	>128	>128	>128
	JI-20A	>128	>128	2	1	>128	>128	>128	16
	GB	>128	>128	4	4	>128	>128	>128	32
	2′DGX2	>128	>128	>128	>128	>128	>128	>128	>128

MIC: minimal inhibitory concentration. Type strains and clinical isolates were obtained from the American Type Culture Collection (ATCC, USA) and the Culture Collection of Antimicrobial Resistant Microbes (CCARM, Republic of Korea), respectively.

Supplementary Table 4. List of bacterial strains and plasmids used in this study

Strain/Plasmid	Relevant characteristics	Reference
Escherichia coli		
DH5α	Host for general cloning	New England Biolabs
BL21(DE3)	Host for recombinant protein expression	Novagen
BL21(DE3)pLysS	Host for recombinant protein expression	Novagen
ArcticExpress(DE3)	Host for recombinant protein expression	Agilent Technologies
Rosetta gami^{TM2}(DE3)	Host for recombinant protein expression	Novagen
ArcticExpress(DE3)/pGENM1	Strain for GenM1 protein expression	This study
BL21(DE3)/pGEND2	Strain for GenD2 protein expression	This study
BL21(DE3)pLysS/pGENS2	Strain for GenS2 protein expression	This study
BL21(DE3)/pGENN	Strain for GenN protein expression	This study
BL21(DE3)pLysS/pGEND1	Strain for GenD1 protein expression	This study
Rosetta gami^{TM2}(DE3)/pGENQ	Strain for GenQ protein expression	This study
BL21(DE3)pLysS/pGENB1	Strain for GenB1 protein expression	This study
BL21(DE3)/pGENJ	Strain for GenJ protein expression	This study
BL21(DE3)/pGENK2	Strain for GenK2 protein expression	This study
BL21(DE3)/pGENB1_D345L	Strain for Asp345 to Leu345 mutant of GenB1 (D345L)	This study
BL21(DE3)/pGENB1_D395L	Strain for Asp395 to Leu395 mutant of GenB1 (D395L)	This study

BL21(DE3)/pGENB1_W391A	Strain for Trp391 to Ala391 mutant of GenB1 (W391A)	This study
BL21(DE3)/pGENB1_W415A	Strain for Trp415 to Ala415 mutant of GenB1 (W415A)	This study
Streptomyces venezuelae		
ATCC 15439	Host for recombinant protein expression	Song, J.Y. *et al.*[1]
S. venezuelae/pGENM2	Strain for GenM2 protein expression	This study
Micromonospora echinospora		
ATCC 15835	Gentamicin producing wild-type strain	Weinstein, M.J. *et al*.[2]
Plasmid		
pGEM-Teasy	PCR fragment cloning vector	Promega
pET15b, pET28a	*E. coli* protein expression vector	Novagen
pJ404	*E. coli* protein expression vector	DNA2.0
pSE34	pWHM3 with P*ermE** promoter	Smirnova, N. & Reynolds, K.A.[3]
pGENM1	N,C-terminal His-tagged GenM1 expression plasmid based on pET28a(+)	This study
pGENM2	N,C-terminal His-tagged GenM2 expression plasmid based on pSE34	This study
pGEND2	N-terminal His-tagged GenD2 expression plasmid based on pJ404	This study
pGENS2	N-terminal His-tagged GenS2 expression plasmid based on pET15b(+)	This study
pGENN	N-terminal His-tagged GenN expression plasmid based on pJ404	This study
pGEND1	N-terminal His-tagged GenD1 expression plasmid based on pET15b(+)	This study
pGENQ	N-terminal His-tagged GenQ expression plasmid based on pET28a(+)	This study

pGENB1	N-terminal His-tagged GenB1 expression plasmid based on pET15b(+)	This study
pGENJ	N-terminal His-tagged GenJ expression plasmid based on pET28a(+)	This study
pGENK2	N,C-terminal His-tagged GenK2 expression plasmid based on pET28a(+)	This study
pGENB1_D345L	N-terminal His-tagged GenB1_D345L mutant expression plasmid based on pET15b(+)	This study
pGENB1_D395L	N-terminal His-tagged GenB1_D395L mutant expression plasmid based on pET15b(+)	This study
pGENB1_W391A	N-terminal His-tagged GenB1_W391A mutant expression plasmid based on pET15b(+)	This study
pGENB1_W415A	N-terminal His-tagged GenB1_W415A mutant expression plasmid based on pET15b(+)	This study

Supplementary Table 5. List of oligonucleotide primers used in this study

Primer	Oligonucleotide sequences (5' to 3', restriction site underlined)	Description
GenM2-F	ATATCATATGGGCGGCATGCACGTGTTG	For protein expression
GenM2-R	ATAGAAGCTTGGACTCCTCCATGAGGGA	For protein expression
GenQ-F	CCCAACCCGGCATATGCTCATCAGCGTTTC	For protein expression
GenQ-R	TTGCCGGCACCGAATTCGATGGTCATCGTG	For protein expression
GenJ-F	AATCTCATATGGTGA AGCCGGCCTCC	For protein expression
GenJ-R	CAGGTCTCGAGTCATTGGATCGCG	For protein expression
GenK2-F	GCCCATATGCCTTCGCGATCCAAT	For protein expression
GenK2-R	TATCTCGAGCGACGACCCGTCG	For protein expression
GenM1-RT1	ATCCGTTCCGAGATCCACT	For RT-PCR
GenM1-RT2	CCGATGTAGCCGATGAGC	For RT-PCR
GenM2-RT1	AGTACGTCATCCAGCACTCC	For RT-PCR
GenM2-RT2	CATGTACTCCAGGACGACGA	For RT-PCR
GenP-RT1	GTTGTCGAGGCAGAAGTC	For RT-PCR
GenP-RT2	GTTCCCTCCTTCTACGTGAA	For RT-PCR
GenK-RT1	ATCATGTCACCGGCGAAG	For RT-PCR
GenK-RT2	CCCGTTCTACCCGATCTA	For RT-PCR
GenE-RT1	AGGGTTACGAGTCCTGGG	For RT-PCR
GenE-RT2	GAACACGACGTCCACCTT	For RT-PCR
GenN-RT1	TTGGTACGTCGACCCGCT	For RT-PCR
GenN-RT2	CTGCGAGGTGAAGATCTGCA	For RT-PCR
GenK2-RT1	ATGCGGTGGTGGATCTGAC	For RT-PCR
GenK2-RT2	ACGGTCCGGTACAGGTCA	For RT-PCR
GenJ-RT1	CAGGTCATCACTCGATCTTC	For RT-PCR
GenJ-RT2	GTTGTGCACGGTGAAGTC	For RT-PCR
GenB1_D345L_P1	GTTTTTCGAGGGTCTTAATCA AACCCCGA	For mutagenesis
GenB1_D345L_P2	TCGGGGTTTGATTAAGACCCTCGAAAAAC	For mutagenesis
GenB1_D395L_P1	GCGCGTGGGGTGCGATGCTCGGCCTGGCGG	For mutagenesis

GenB1_D395L_P2	CCGCCAGGCCGAGCATCGCACCCCACGCGC	For mutagenesis
GenB1_W391L_P1	GCTGGTACGCCAGCGCGGCGGGTGCGATGGACGGCC	For mutagenesis
GenB1_W391L_P2	GGCCGTCCATCGCACCCGCCGCGCTGGCGTACCAGC	For mutagenesis
GenB1_W415L_P1	ATTGTGGAGCGTCTGGCGGAAGATTAACTCGAG	For mutagenesis
GenB1_W415L_P2	CTCGAGTTAATCTTCCGCCAGACGCTCCACAAT	For mutagenesis

References

1. Song, J.Y. et al. Complete genome sequence of *Streptomyces venezuelae* ATCC 15439, a promising cell factory for production of secondary metabolites. *J. Biotechnol*. **219**, 57–58 (2016).
2. Weinstein, M.J. *et al*. Gentamicin, a new antibiotic complex from *Micromonospora*. *J. Med. Chem.* **6**, 463–464 (1963).
3. Smirnova, N. & Reynolds, K.A. Engineered fatty acid biosynthesis in Streptomyces by altered catalytic function of β-ketoacyl-acyl carrier protein synthase III. *J. Bacteriol.* **183**, 2335–2342 (2001).